

## CHAPTER 5

### Phosphonate- and Carboxylate-Based Chelating Agents that Solubilize (Hydr)oxide-Bound $\text{Mn}^{\text{III}}$

#### 5.1 Abstract

This study examines  $\text{Mn}^{\text{III}}$  solubilization from a synthetic  $\text{MnO}_2$ (birnessite), which contains one-fifth of  $\text{Mn}^{\text{III}}$ , and a synthetic  $\text{MnOOH}$ (manganite), which contains solely  $\text{Mn}^{\text{III}}$ , by two groups of chelating agents in large excess with respect to oxide concentration in circum-neutral solutions, using the measurement of total dissolved Mn ( $\text{Mn}_{\text{T}}(\text{aq})$ ) and  $\text{Mn}^{\text{III}}$  ( $\text{Mn}^{\text{III}}(\text{aq})$ ). For reaction of the two oxides with inorganic pyrophosphate (PP) and five related phosphonate- and carboxylate-containing chelating agents, MP, EDP, and PPA do not cause discernable dissolution. PP, MDP and PAA yield  $\text{Mn}^{\text{III}}(\text{aq})$  as the predominant  $\text{Mn}_{\text{T}}(\text{aq})$  species, regardless of pH, chelating agent concentration and oxide loading, although at different rates and to a different extent. Since PP, MDP and PAA are not oxidized by  $\text{Mn}^{\text{III}}$  within timescales of each dissolution experiment,  $\text{Mn}^{\text{III}}(\text{aq})$  production arises from ligand-assisted dissolution. The typical dissolution profile exhibits an initial fast dissolution and later dissolution slows down over time. Comparing PP and MDP, PAA solubilizes  $\text{Mn}^{\text{III}}$  to a significantly lesser extent. For reaction of  $\text{MnOOH}$  with four aminophosphonate- and aminocarboxylate-containing ligands, IDMP causes primarily ligand-assisted dissolution; PMG causes both ligand-assisted dissolution and reductive dissolution; MIDA causes reductive dissolution only; IDA does not contribute to dissolution.

## 5.2 Introduction

There is a great deal of recent interest in the possible role that dissolved  $\text{Mn}^{\text{III}}$  may play in biogeochemical redox processes (1-9). Fungal production of dissolved  $\text{Mn}^{\text{III}}$  complexes from the oxidation of  $\text{Mn}^{\text{II}}$  complexes with malonate, malate, gluconate, glucuronate, and other (hydroxy)carboxylate chelating agents, and subsequent oxidative breakdown of lignin is now well established (10-12). More recently,  $\text{Mn}^{\text{III}}$  complexes with bacterial siderophores such as pyoverdine (6) and desferrioxamine B (7, 8) have been investigated. Dissolved extracellular  $\text{Mn}^{\text{III}}$  can oxidize a wide range of inorganic and organic species in environmental media.  $\text{Mn}^{\text{III}}$  taken up by organisms can be quite toxic.

Water treatment processes add chlorine, ozone, or other chemical oxidants prior to filtration, which cause Mn oxidation and precipitation onto filter media (13). Sporadic Mn release from filters is difficult to prevent and poorly understood. Although re-reduction to soluble  $\text{Mn}^{\text{II}}$  is the likely cause,  $\text{Mn}^{\text{III}}$  dissolution merits consideration too. Power plant cooling water systems employ chlorine to control biofouling. In such systems,  $\text{Mn}^{\text{II}}$  in source waters is oxidized to  $\text{Mn}^{\text{III,IV}}$  (hydr)oxides, which coat pipe walls (14). Chemical additives used in engineered systems (e.g. coagulant aids, anti-corrosion agents, scale-control agents) should be scrutinized for their ability to solubilize  $\text{Mn}^{\text{III}}$ .

Synthetic chelating agents that are intentionally or inadvertently released into environmental media have the potential of solubilizing  $\text{Mn}^{\text{III}}$ . The herbicide glyphosate possesses three Lewis Base groups (amine, phosphonate, carboxylate) suitably placed for chelating  $\text{Fe}^{\text{III}}$  (15, 16) and by inference other +III metal ions. U.S. glyphosate use in 2001 was approximately 40 million kilograms (17), more than any other agrochemical active ingredient. Chelating agents used for water hardness control (e.g. pyrophosphate

and nitrilotrimethylenephosphonate (NTMP)) and pharmaceuticals with chelating agent properties (e.g. antiviral compounds such as phosphonoformate and phosphonoacetate, and bone loss preventatives such as the bis-diphosphonates fosamax and clodronate) are present in residential wastewaters, and can enter soils through the land application of biosolids and the use of septic tank/leachfield systems. Commercial laundries, paper and textile manufacturers, and a wide range of other industries release carboxylate- and phosphonate-based chelating agents into wastewaters, which are only partially removed during treatment (e.g. Nowack (18); Ridge and Sedlak (19)). Phosphonate-based chelating agents are injected into oil and natural gas fields to prevent  $\text{BaSO}_4(\text{s})$  scale formation (20).

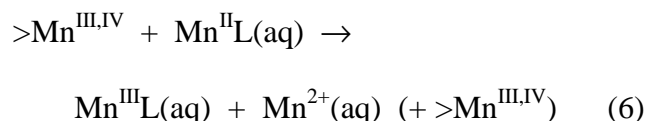
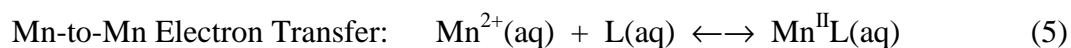
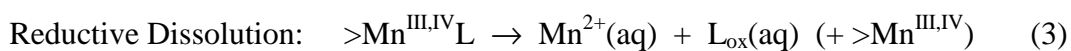
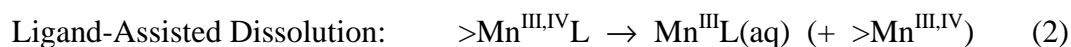
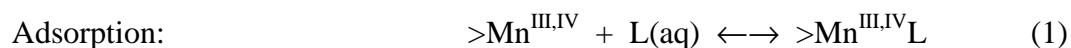
Prior studies used absorbance in the 400 - 500 nm range to detect dissolved  $\text{Mn}^{\text{III}}$ , yielding a detection limit of approx. 20  $\mu\text{M}$ . Reaction of hydroxyethane-1,1-diphosphonate (HEDP) with a synthetic  $\text{MnO}_2(\text{s})$  has been reported to yield dissolved  $\text{Mn}^{\text{III}}$  (21). Considerable quantities of dissolved  $\text{Mn}^{\text{III}}$  were observed when pyrophosphate and citrate were brought into contact with a (hydr)oxide phase consisting primarily of  $\text{Mn}^{\text{III}}$  (4). Above pH 6.5, reaction of desferrioxamine B with  $\text{MnOOH}$ (manganite) produces dissolved  $\text{Mn}^{\text{III}}$  exclusively, but below pH 6.5, a mixture of dissolved  $\text{Mn}^{\text{II}}$  and  $\text{Mn}^{\text{III}}$  is obtained (8). It is noteworthy that  $> 20 \mu\text{M}$  concentrations of dissolved  $\text{Mn}^{\text{III}}$  were not observed in the reaction of EDTA (4, 22) and NTMP (23) with (hydr)oxides consisting primarily of  $\text{Mn}^{\text{III}}$ .

Capillary electrophoresis (CE) with a pH 7.0 capillary electrolyte comprising pyrophosphate, orthophosphate, and tetradecyltrimethylammonium bromide (TTAB) has recently enabled us to lower the detection limit for dissolved  $\text{Mn}^{\text{III}}$  with weak-to-

moderate strength chelating agents to 1.5  $\mu\text{M}$  (Chapter 2). Using this technique, dissolved  $\text{Mn}^{\text{III}}$  concentrations in the 2.0 to 5.0  $\mu\text{M}$  range were observed when a 200  $\mu\text{M}$  citrate solution was reacted with 200  $\mu\text{M}$   $\text{MnO}_2$ (birnessite). This phase contains 22 %  $\text{Mn}^{\text{III}}$ , and hence some of the dissolved  $\text{Mn}^{\text{III}}$  may have come from ligand-assisted dissolution. A significant lag period was observed, however, which was eliminated by addition of 10  $\mu\text{M}$   $\text{Mn}^{\text{II}}$ . This observation suggests that the oxidation of  $\text{Mn}^{\text{II}}$ -citrate complexes by  $\text{MnO}_2(\text{s})$  is also taking place.

We have also recently reported (Chapter 3) that 5.0 mM phosphonoformate at pH 7.0 dissolves  $\text{MnOOH}$ (manganite) exclusively through a ligand-assisted dissolution pathway. Lowering the pH to 6.0 and 5.0 shifts dissolved Mn from solely the +III oxidation state to a mixture of +II and +III oxidation states. Reaction with the  $\text{MnO}_2$ (birnessite) phase yielded only  $\text{Mn}^{\text{II}}$ .

Whenever a chelating agent is brought into contact with a  $\text{Mn}^{\text{III,IV}}$  (hydr)oxide phase, the following reaction pathways are potentially available:

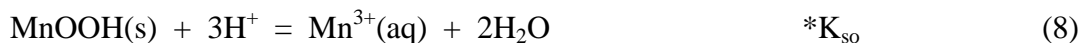




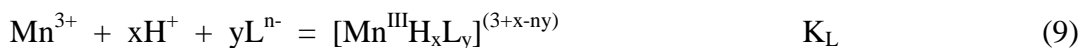
Reactions 5 and 6, if significant, will yield an autocatalytic time course plot. Reaction 3, reductive dissolution, is a competitive pathway that works against dissolved  $\text{Mn}^{\text{III}}$  production. Reaction 4 represents a sink for dissolved  $\text{Mn}^{\text{III}}$ . Hence, if appreciable dissolved  $\text{Mn}^{\text{III}}$  is to be observed, rate constants for Reactions 1 and 2 must be large relative to rate constants for Reactions 3 and 4. Ligand-assisted dissolution reactions are generally believed to be proportional to the extent of chelating agent adsorption (24). Using  $\text{Mn}^{\text{III}}(\text{aq})$  to denote the total dissolved  $\text{Mn}^{\text{III}}$  concentration, we can write:

$$R_L = \frac{d\text{Mn}^{\text{III}}(\text{aq})}{dt} = k_L[>\text{Mn}^{\text{III,IV}}\text{L}] = k_L C_L^s \quad (7)$$

In addition to these kinetic descriptions, thermodynamics places important constraints on whether or not dissolved  $\text{Mn}^{\text{III}}$  can be observed. Because we do not have thermodynamic information for the 22 %  $\text{Mn}^{\text{III}}$  found within our  $\text{MnO}_2$ (birnessite) phase (Chapter 2), we will use  $\text{MnOOH}$ (manganite) as the solubility-limiting phase throughout this discussion. We use  $*K_{\text{so}} = 10^{-1.20}$  for the solubility constant for the reaction given below (see Chapter 2, Supporting Information).



If we use  $\text{L}^{n-}$  to represent the chelating agent in its lowest protonation level, then the following generic equation encompassing all potential stoichiometries and protonation levels for dissolved  $\text{Mn}^{\text{III}}$  species can be written:



Adding these two reactions together yields:



From this reaction it follows that the dissolved  $\text{Mn}^{\text{III}}$  concentration achieved when saturation with respect to  $\text{MnOOH}$ (manganite) has been obtained depends upon the magnitude of the complex formation constant ( $K_L$ ) and the chelating agent concentration:

$$[\text{Mn}^{\text{III}}\text{H}_x\text{L}_y]^{(3+x-ny)} = *K_{\text{so}}K_L[\text{H}^+]^{(3+x)}[\text{L}^{\text{n-}}]^y a_{\text{MnOOH}} \quad (11)$$

A low value of  $K_L$  can be compensated by a high total chelating agent concentration (TOTL). pH is also an important consideration, since protons compete with  $\text{Mn}^{\text{III}}$  for available chelating agent, and the chelating agent competes with hydroxide ions for  $\text{Mn}^{\text{III}}$ .

Mass balance equations for  $\text{Mn}^{\text{III,IV}}$  (hydr)oxide surface sites and for chelating agent are also relevant to ligand-assisted dissolution reactions:

$$S_T = [>\text{Mn}^{\text{III,IV}}] + [>\text{Mn}^{\text{III,IV}}\text{L}] \quad (12)$$

$$\text{TOTL} = [>\text{Mn}^{\text{III,IV}}\text{L}] + [\text{L}_{\text{free}}(\text{aq})] + [\text{Mn}^{\text{III}}\text{-L}(\text{aq})] \quad (13)$$

Lin and Benjamin (25) pointed out that a special situation exists when the adsorption constant corresponding to Reaction 1 (which we will denote as  $K_{\text{ads}}$ ) is large and  $S_T \geq \text{TOTL}$ .  $[>\text{Mn}^{\text{III,IV}}\text{L}]$ , the first term in Equation 13, becomes large relative to the other two terms. Ligand-assisted dissolution cannot hence take place because the dissolved ligand concentration ( $L_T = [\text{L}_{\text{free}}(\text{aq})] + [\text{Mn}^{\text{III}}\text{-L}(\text{aq})]$ ) is not high enough.

Another special situation deserves attention. If  $\text{TOTL} \geq S_T$  and if  $K_{\text{ads}}$  is large, saturation of the surface with adsorbed chelating agent takes place. Dissolution will occur, but according to Equation 7, the dissolution rate should be independent of the added chelating agent concentration.

The objectives of our present work are to (i) survey a number of carboxylate- and phosphonate-based chelating agents (Table 5.1) regarding their ability to solubilize  $\text{Mn}^{\text{III}}$ , (ii) compare ligand-assisted dissolution reactions of  $\text{MnOOH}$ (manganite) with those of

MnO<sub>2</sub>(birnessite), and (iii) use rates and extent of dissolution as a function of chelating agent concentration and pH to learn more about reaction mechanisms responsible for dissolved Mn<sup>III</sup> production.

### 5.3 Materials and Methods

All solutions were prepared from reagent grade chemicals without further purification, and distilled, deionized water (DDW) with a resistivity of 18 M $\Omega$ -cm (Millipore Corp., Milford, MA). Filter holders (Whatman Scientific, Maidstone, England) were soaked in 1N ascorbic acid (Aldrich, Milwaukee, WI) and rinsed with distilled water and DDW. All bottles and glassware for MnO<sub>2</sub>(birnessite) and MnOOH(manganite) suspensions were first soaked in 1N ascorbic acid and rinsed with distilled water; and were next put in a 4N nitric acid (J. T. Baker, Phillipsburg, NJ) bath overnight and rinsed with distilled water and DDW water prior to use.

**5.3.1 Chemicals.** Phosphonoacetic acid (PAA), methyliminodiacetic acid (MIDA), and Mn<sup>III</sup>(acetate)<sub>3</sub>·2H<sub>2</sub>O were purchased from Aldrich. Iminodi(methylphosphonic acid) (IDMP), di-sodium dihydrogen pyrophosphate (PP), methylphosphonic acid (MP), and N-(phosphonomethyl)glycine (PMG) were purchased from Fluka (Buchs, Switzerland). Iminodiacetic acid (IDA) was purchased from Sigma (St Louis, MO). 3-Phosphonopropionic acid (PPA) and 1,2-ethylenediphosphonic acid (EDP) were purchased from Lancaster Synthesis (Windham, NH). Methylenediphosphonic acid (MDP) was purchased from Alfa Aesar (Ward Hill, MA). 2-Phosphonobutane-1,2,4-tricarboxylic acid (PBTC) was purchased from Halag Chemie

AG (Aadorf, Switzerland). HNO<sub>3</sub> (nitric acid), HCl (hydrochloric acid), NaOH (sodium hydroxide), and NaCl (sodium chloride) were purchased from J. T. Baker.

Our Mn<sup>III</sup>-pyrophosphate stock solution contained a 20-fold excess of pyrophosphate. 13.4 mg Mn<sup>III</sup>(acetate)<sub>3</sub>·2H<sub>2</sub>O was dissolved in 50 mLs of a 20 mM disodium pyrophosphate solution that had been previously adjusted to pH 7 using NaOH addition. After dissolution was complete, the pH was again adjusted to pH 7. The solution was then filtered using a 0.1 µm pore size etch-tracked polycarbonate membrane (Whatman Scientific). Total dissolved Mn was determined in the filtered solution using flame atomic absorption spectrophotometry (AAS: Aanalyst 100, Perkin Elmer, Norwalk, CT). Following the method of Kostka et al. (2), dissolved Mn<sup>III</sup> was determined in this solution by UV-visible spectrophotometry (model UV-160U, Shimadzu Instrument Co., Kyoto, Japan) at a wavelength of 480 nm (molar absorptivity = 110 cm<sup>-1</sup> M<sup>-1</sup>). The Mn<sup>III</sup>-pyrophosphate solution was stable enough to serve as a capillary electrophoresis (CE) standard for dissolved Mn<sup>III</sup>. The solution was stored in a 4 °C refrigerator and remade every two weeks.

MnO<sub>2</sub> herein refers to particles synthesized according to the method of Luo et al. (26); details of the synthesis and characterization are provided elsewhere (27).

Diffraction lines obtained by X-ray diffraction are consistent with a distorted birnessite layered structure. Transmission electron microscopy revealed many of the MnO<sub>2</sub> sheets were curled, which was attributed to edge sections thicker than middle sections (Figure 5.1a). A B.E.T. surface area of 174 m<sup>2</sup>/g was determined using a freeze-dried sample. The average Mn oxidation state was found to be +3.78 based upon iodometric titration. If the assumption is made that the Mn<sup>II</sup> content is negligible, then the (hydr)oxide

consists of a mixture of 22 %  $\text{Mn}^{\text{III}}$  and 78 %  $\text{Mn}^{\text{IV}}$ . The freeze-dried particles weighed 97.10 grams per mole of manganese.

$\text{MnOOH}$  herein refers to particles synthesized according to the method of Giovanoli and Leuenberger (28); details of the synthesis and characterization are provided elsewhere (29). Diffraction lines obtained by X-ray diffraction are consistent with the mineral manganite structure. Transmission electron microscopy revealed needle-shaped crystals of uniform size (Figure 5.1b). The average Mn oxidation state for a predominantly manganite phase should be close to +3.0. A B.E.T. surface area of 27.3  $\text{m}^2/\text{g}$  was determined using a freeze-dried sample. The freeze-dried particles weighed 91.5 grams per mole of manganese.

**5.3.2 Experimental Setup.** All dissolution experiments were conducted in 100 mL polypropylene bottles in a constant temperature circulating bath at  $25 \pm 0.2$  °C and stirred with Teflon-coated stir bars. Solutions containing ligand (plus additional constituents, as appropriate) were sparged with Ar (BOC gases, Baltimore, MD) for one hour prior to  $\text{MnO}_2$  or  $\text{MnOOH}$  addition. Sparging was continued during the duration of the experiments. pH was monitored during each reaction using a Fisher Accumet AR15 meter with Orion combination semi-micro glass electrode and NIST-traceable standard buffer solutions. In some experiments, one or more  $\text{pK}_{\text{a}}$ s of the chelating agent were close enough to the desired pH and the chelating agent concentration was high enough to maintain constant pH throughout the reaction time course. We will refer to this as "self-buffering". In other experiments, additions of strong acid (HCl) or strong base (NaOH) were necessary during the reaction time course. A computer-controlled system consisting

of two burettes, pH meter, and controlling software, termed a pH-stat, was used for this purpose.

Reaction suspension aliquots of 4 mL were collected at periodic intervals.

Reactions were quenched by immediately filtering through 0.1  $\mu\text{m}$  pore diameter track-etched polycarbonate filter membranes (Whatman). Total dissolved manganese ( $\text{Mn}_{\text{T}}(\text{aq})$ ) in the filtered solutions was analyzed using flame atomic absorption spectrophotometry (AAS: Aanalyst 100, Perkin Elmer, Norwalk, CT). Dissolved  $\text{Mn}^{\text{III}}(\text{Mn}^{\text{III}}(\text{aq}))$  in the filtered solutions was analyzed using capillary electrophoresis (see next section).

**5.3.3 Capillary Electrophoresis:  $\text{Mn}^{\text{III}}(\text{aq})$  Analysis.** A capillary electrophoresis unit from Beckman Coulter (P/ACE MDQ, Fullerton, CA) with diode-array UV-visible detector was used for all determinations. Detector bandwidth was set at 6 nm for 190 nm wavelength detection and 10 nm for all other wavelengths. Bare fused silica capillaries (Polymicro Technologies, Phoenix, AZ) with 75  $\mu\text{m}$  ID  $\times$  60 cm total length were used for all separations. The effective length defined as the length from the inlet to the detector was 52 cm. Capillary and sample board temperature was thermostatted to 10  $^{\circ}\text{C}$  during operation. Between separations, the capillary was sequentially rinsed by flushing DDW for 0.5 minute, 0.1 M NaOH for 1 minute, DDW again for 1 minute, and capillary electrolyte for 2 minutes. Sample injection employed 0.5 psi of positive pressure for 15 seconds. Anion mode with constant applied voltage (-22 kV) was employed for all separations.

In previous efforts to obtain metal ion and chelating agent speciation information (30) a non-complexing CE electrolyte such as 50 mM MOPS (pH 7.0) and 0.5 mM TTAB was employed. Using this CE electrolyte with  $\text{Mn}^{\text{III}}$ -pyrophosphate solutions,

however, yielded a baseline increase and a broad, unusable peak. When  $\text{Mn}^{\text{II}}$ -containing stock solutions were injected, no peak was obtained. Measured currents declined with successive injections, which we conclude was caused by formation of inorganic precipitates, leading to column clogging. The unusable or undetectable peaks are likely caused by ligand exchange during electromigration, which is reasonable based upon the fact that  $\text{Mn}^{3+}$  is more substitution-labile than other +III metal ions and  $\text{Mn}^{2+}$  is more substitution-labile than other +II metal ions that we have worked with in the past (30, 31). Since the CE electrolyte does not contain ligands capable of solubilizing  $\text{Mn}^{\text{III}}$ , any electric field-induced dissociation will lead to  $\text{Mn}^{\text{III}}$  precipitation within the column. Precipitation of  $\text{Mn}^{\text{II}}$  within the column is harder to explain, but may involve precipitation with inorganic carbonate, inadvertently introduced to the CE electrolyte through contact with air.

We elected to use a CE electrolyte consisting of 20 mM pyrophosphate, 0.4 mM TTAB, and 2 mM orthophosphate (pH 9.5) for our CE determinations. For filtered reaction solutions from Group I chelating agents (Table 5.1)-containing Mn (hydr)oxide suspensions, pyrophosphate was a strong enough chelating agent for  $\text{Mn}^{\text{III}}$  and present in a high enough concentration to capture all the  $\text{Mn}^{\text{III}}$  in our samples during electromigration. A sharp, symmetrical peak, easily discernable at a detection wavelength of 235 nm, provided the means of measuring  $\text{Mn}^{\text{III}}(\text{aq})$  (total dissolved  $\text{Mn}^{\text{III}}$ ). The detection limit for  $\text{Mn}^{\text{III}}(\text{aq})$  was about 1.5  $\mu\text{M}$  at this wavelength. For filtered reaction solutions from Group II chelating agents (Table 5.1)-containing Mn (hydr)oxide suspensions, however, pyrophosphate was not a strong enough chelating agent to replace Group II chelating agents from the  $\text{Mn}^{\text{III}}$  complexes during electromigration. In this case,

it was not appropriate to calculate  $\text{Mn}^{\text{III}}$  concentrations in the filtered reaction solutions based upon calibration curves obtained from  $\text{Mn}^{\text{III}}$ -pyrophosphate standard solutions. A rough  $\text{Mn}^{\text{III}}$  quantification was done by calculating the ratio of peak area over migration time, where a high value of the ratio corresponded to a high  $\text{Mn}^{\text{III}}$  concentration, and vice versa.

LogK values for  $\text{Mn}^{\text{II}}$  complexes with pyrophosphate are significantly lower than those for  $\text{Mn}^{\text{III}}$  (32, 33). The sharpest, most symmetrical peak for  $\text{Mn}^{\text{II}}$  is obtained when a CE electrolyte with a pH of 9.5 is employed. Lowering the pH of the CE electrolyte causes more and more peak broadening and tailing, and an increase in the baseline. The  $\text{Mn}^{\text{II}}(\text{aq})$  peak is more discernable at 214 nm than at 235 nm, consistent with its known spectral qualities (32). Although no attempt was made to quantify  $\text{Mn}^{\text{II}}$  using CE, the pyrophosphate-TTAB-orthophosphate CE electrolyte did succeed in preventing measured current decline and increasing column life, especially at pH 9.5.

## 5.4 Results

**5.4.1 Dissolution of  $\text{MnO}_2$  by PP, MDP and PAA in Group I Chelating Agents.** As shown in Table 5.1, group I chelating agents bear carboxylate group and/or phosphonate or phosphate group. Dissolution of  $\text{MnO}_2$  by PP, MDP, and PAA has been investigated under various reaction conditions, including pH, chelating agent concentration, and surface loading (Figures 5.2 to 5.5). For all reactions,  $\text{Mn}_{\text{T}}(\text{aq})$  (total dissolved Mn) measured by AAS and  $\text{Mn}^{\text{III}}(\text{aq})$  (dissolved  $\text{Mn}^{\text{III}}$ ) measured by CE are equal. All reaction time courses exhibit the initial fast release of  $\text{Mn}^{\text{III}}(\text{aq})$  followed by a much slower release stage. In order to observe the eventual leveling out of concentration, it is



necessary to monitor the experiments for 25 hours. To make quantitative run-to-run comparisons, we have selected to calculate two guidepost ratios ( $\text{Mn}^{\text{III}}(\text{aq})/\text{TOTMn}^{\text{III}}$ ): after 20 minutes and after 20 hours of reaction, in order to illustrate the initial fast dissolution and the later leveling out stage, respectively. Note that the  $\text{MnO}_2$  preparation used in our experiments consists of 22% of  $\text{Mn}^{\text{III}}$ , and hence loadings of 200 and 500  $\mu\text{M}$  of suspension correspond to 44 and 110  $\mu\text{M}$  of  $\text{TOTMn}^{\text{III}}$ , respectively.

Time course plots at different pHs for reactions employing 200  $\mu\text{M}$  of oxide loading and 5.0 mM of chelating agents (PP, MDP and PAA) are presented in Figure 5.2. For all time course experiments, the guidepost ratio  $\text{Mn}^{\text{III}}(\text{aq})/\text{TOTMn}^{\text{III}}$  after 20 minutes and 20 hours of reaction, referred to the initial ratio and the later ratio, are presented in Figure 5.3a. With PP, the initial ratio decreases from near 0.5 to 0.2 as raising pH from 5.0 to 7.0, and remains at 0.2 as further raising pH to 8.0. The later ratios are close to 1.0 at all pHs, with the pH 5.0 value slightly lower than the pH 6.0, 7.0 and 8.0 value. The average Mn oxidation state of  $\text{MnO}_2$  suspensions goes up from +3.78 at the onset of reaction to 3.96 after all  $\text{TOTMn}^{\text{III}}$  is released to solution. With MDP, a trend of decreasing the initial ratio from 0.40 to 0.15 as increasing pH matches that of PP, in spite of a slightly lower ratio at each pH. The later ratio matches that of PP only at pH 5.0 (close to 1.0), but decreases to near 0.65 at pH 6.0, 7.0 and 8.0. With PAA, at pH 5.0, the initial ratio and the later ratio are one-half of those of PP and MDP. Increasing pH to 6.0 and 7.0 causes both ratios to decrease continuously. Upon further increasing pH to 8.0, the reaction shuts off completely.

Effect of PP, MDP and PAA concentration (from 1.0 to 100 mM) on reaction time course plots at pH 7.0 (200  $\mu\text{M}$   $\text{MnO}_2$ ) is presented in Figure 5.4a and b. The

corresponding guidepost ratios ( $\text{Mn}^{\text{III}}(\text{aq})/\text{TOTMn}^{\text{III}}$ ) at different PP, MDP and PAA concentrations are presented in Figure 5.4c. With PP, the initial ratio increases from near 0.05 to 0.42 in raising PP concentration from 1.0 to 100 mM. The increase in initial ratio levels out at higher PP concentration. The PP concentration effect on the later ratio is unexpected: giving 0.05 with 1.0 mM PP, and near 0.8 with 5.0 up to 100 mM PP. With MDP, both initial ratio and later ratio increase as increasing MDP concentration, and level out at higher MDP concentration. 20 mM MDP is enough to dissolve all of  $\text{TOTMn}^{\text{III}}$  after 20 hours of reaction. With PAA, the general trend of concentration effect matches that of MDP, but the ratios are lower at the same chelating agent concentration. 100 mM PAA dissolves 0.86 of  $\text{TOTMn}^{\text{III}}$  after 20 hours of reaction.

As shown in Figure 5.5, a 2.5-fold increase in  $\text{MnO}_2$  loading (from 200 to 500  $\mu\text{M}$ ) yields very similar time course plots with respect to  $\text{Mn}^{\text{III}}(\text{aq})/\text{TOTMn}^{\text{III}}$  for experiments employing 5.0 mM PP, MDP and PAA, at pH 6.0. A 2.5-fold increase in  $\text{MnO}_2$  loading corresponds to a 2.5-fold increase in  $\text{TOTMn}^{\text{III}}$ . Therefore, the increase in loading causes a 2.5-fold increase in  $\text{Mn}^{\text{III}}(\text{aq})$  production throughout the reaction time course.

It is worth mentioning that both Figures 5.2 and 5.4 include the time course plots for reaction of 5.0 mM PP, MDP and PAA with 200  $\mu\text{M}$   $\text{MnO}_2$  at pH 7.0. However, the experiments presented in Figure 5.4 were performed six months after those presented in Figure 5.2, meaning that the  $\text{MnO}_2$  preparation age is different. Under the reaction conditions, the  $\text{MnO}_2$  aging effect is insignificant within six months of period (Figure S5.1, Supporting Information).

#### 5.4.2 Dissolution of MnOOH by PP, MDP and PAA in Group I Chelating

**Agents.** Time course plots for dissolution of 200  $\mu\text{M}$  MnOOH by 5.0 mM chelating agents (PP, MDP and PAA) at different pHs are presented in Figure 5.6.  $\text{Mn}_{\text{T}}(\text{aq})$  and  $\text{Mn}^{\text{III}}(\text{aq})$  are nearly equal except that, with pH 5.0 experiments,  $\text{Mn}^{\text{III}}(\text{aq})$  is lower than  $\text{Mn}_{\text{T}}(\text{aq})$  to different degrees, depending on the specific chelating agent. As with  $\text{MnO}_2$ , all reaction time courses exhibit an initial fast release of  $\text{Mn}^{\text{III}}(\text{aq})$  followed by a much slower release stage. However, it is necessary to monitor the experiments for 250 hours, instead of 25 hours with  $\text{MnO}_2$ , to observe the eventual leveling out of concentration. Consequently, the two guidepost ratios ( $\text{Mn}^{\text{III}}(\text{aq})/\text{TOTMn}^{\text{III}}$ ) to represent the initial fast dissolution and the later leveling out stage are picked after 200 minutes and 200 hours (see Figure 5.3b), instead of 20 minutes and 20 hours with  $\text{MnO}_2$ . Note that the MnOOH preparation used in our experiments consists predominantly of  $\text{Mn}^{\text{III}}$ , and hence it is reasonable to assume that a loading of 200  $\mu\text{M}$  of suspension corresponds to 200  $\mu\text{M}$  of  $\text{TOTMn}^{\text{III}}$ .

With PP, after 200 minutes of reaction,  $\text{Mn}^{\text{III}}(\text{aq})$  accounts for 0.05 to 0.16 of  $\text{TOTMn}^{\text{III}}$ ; the pH dependence is not significant. After 200 hours of reaction, unlike  $\text{MnO}_2$  dissolution, where pH dependence is insignificant,  $\text{Mn}^{\text{III}}(\text{aq})$  levels out at near 0.4 of  $\text{TOTMn}^{\text{III}}$  at both pH 5.0 and 8.0, but 2.2-times this value at both pH 6.0 and 7.0. Note that  $\text{Mn}^{\text{III}}(\text{aq})$  is lower than  $\text{Mn}_{\text{T}}(\text{aq})$  for pH 5.0 reaction. At the sampling point closest to the 200 hours of reaction,  $\text{Mn}^{\text{III}}(\text{aq})$  is about 80% of  $\text{Mn}_{\text{T}}(\text{aq})$ , corresponding to 20  $\mu\text{M}$  concentration difference.  $\text{Mn}^{\text{III}}(\text{aq})$  equals to  $\text{Mn}_{\text{T}}(\text{aq})$  throughout reaction for reactions at other pHs.

With MDP, after 200 minutes of reaction,  $\text{Mn}^{\text{III}}(\text{aq})/\text{TOTMn}^{\text{III}}$  is lower than that of PP; as for PP, the pH dependence is also not significant. After 200 hours of reaction,  $\text{Mn}^{\text{III}}(\text{aq})$  levels out at near 0.75 of  $\text{TOTMn}^{\text{III}}$  at both pH 5.0 and 6.0. At pH 7.0, leveling out occurs at a concentration that is only one-third this value. At pH 8.0, leveling out occurs at an even lower concentration. Obviously, the observed pH dependence for the leveling out stage of reaction is different from that with  $\text{MnO}_2$ . Note that  $\text{Mn}^{\text{III}}(\text{aq})$  is lower than  $\text{Mn}_{\text{T}}(\text{aq})$  for reaction at pH 5.0. At the sampling point closest to the 200 hours of reaction,  $\text{Mn}^{\text{III}}(\text{aq})$  is about 80% of  $\text{Mn}_{\text{T}}(\text{aq})$ , corresponding to 30  $\mu\text{M}$  concentration difference.  $\text{Mn}^{\text{III}}(\text{aq})$  equals to  $\text{Mn}_{\text{T}}(\text{aq})$  throughout reaction for reactions at other pHs.

With PAA, the dissolution is so slow that no discernable  $\text{Mn}^{\text{III}}(\text{aq})$  is observed in the early stage of reaction (after 200 minutes of reaction), regardless of pH. At pH 5.0, leveling out occurs at a  $\text{Mn}^{\text{III}}(\text{aq})$  concentration that is only 0.1 of  $\text{TOTMn}^{\text{III}}$  over 200 hours of reaction.  $\text{Mn}^{\text{III}}(\text{aq})$  is lower than  $\text{Mn}_{\text{T}}(\text{aq})$ . At the sampling point closest to the 200 hours of reaction,  $\text{Mn}^{\text{III}}(\text{aq})$  is about 55% of  $\text{Mn}_{\text{T}}(\text{aq})$ , corresponding to 15  $\mu\text{M}$  concentration difference. At pH 6.0, leveling out occurs at a lower  $\text{Mn}^{\text{III}}(\text{aq})$  concentration.  $\text{Mn}^{\text{III}}(\text{aq})$  equals to  $\text{Mn}_{\text{T}}(\text{aq})$  throughout the reaction. At pH 7.0 and 8.0, the reaction shuts off completely. Comparing to  $\text{MnO}_2$ , the general trend of pH dependence is similar, but  $\text{MnOOH}$  dissolution is less efficient than that of  $\text{MnO}_2$ .

**5.4.3 Other Group I Chelating Agents.** Unlike PP, MDP, and PAA, which release  $\text{Mn}^{\text{III}}(\text{aq})$  from  $\text{MnO}_2$  and  $\text{MnOOH}$  under certain conditions, MP, EDP and PPA does not yield  $\text{Mn}^{\text{III}}(\text{aq})$  above the detectible level (1.5  $\mu\text{M}$ ) under the same conditions. The release of  $\text{Mn}_{\text{T}}(\text{aq})$  from the oxides in the presence of MP, EDP and PPA is the same as that in the absence of these chelating agents. Assuming the release of  $\text{Mn}_{\text{T}}(\text{aq})$  with

and without chelating agents are parallel processes, MP, EDP and PPA does not contribute to the production of  $\text{Mn}_T(\text{aq})$ .

As shown in Figure 5.7, PBTC does cause  $\text{MnO}_2$  to dissolve. The reaction has been performed employing 5.0 mM PBTC, 200  $\mu\text{M}$   $\text{MnO}_2$ , at pH 5.0. The time course plots show a fast release of  $\text{Mn}^{\text{III}}(\text{aq})$ , where  $\text{Mn}^{\text{III}}(\text{aq})$  equals  $\text{Mn}_T(\text{aq})$ , in the initial stage of reaction. As reaction proceeds further,  $\text{Mn}^{\text{III}}(\text{aq})$  levels out at approximately 10  $\mu\text{M}$ .  $\text{Mn}_T(\text{aq})$ , however, continues to increase gradually, at a rate of  $4.8 \times 10^{-1} \mu\text{M/h}$ . At the last sampling point,  $\text{Mn}_T(\text{aq})$  is 55  $\mu\text{M}$ , higher than  $\text{TOTMn}^{\text{III}}$  (44  $\mu\text{M}$ ) for a 200  $\mu\text{M}$   $\text{MnO}_2$  suspension, indicating that some portion of the  $\text{Mn}_T(\text{aq})$  is from  $\text{Mn}^{\text{IV}}$  content in the  $\text{MnO}_2$  suspension.

**5.4.4 Dissolution of  $\text{MnOOH}$  by Group II Chelating Agents.** As shown in Table 5.1, group II chelating agents bear an aminocarboxylate group and/or aminophosphonate group. Figure 5.8a presents time course plots for dissolution of 200  $\mu\text{M}$   $\text{MnOOH}$  by 5.0 mM chelating agents at pH 6.0 with respect to  $\text{Mn}_T(\text{aq})$  production (top panel) and  $\text{Mn}^{\text{III}}(\text{aq})$  production (bottom panel). Note that  $\text{Mn}^{\text{III}}(\text{aq})$  is represented by the ratio of CE peak area over migration time, in unit of “time corr. peak area”. Referring back to  $\text{Mn}^{\text{III}}$  quantification discussed in the Materials and Methods section, a higher value of this ratio corresponds to a higher  $\text{Mn}^{\text{III}}$  concentration.

What can we say about  $\text{Mn}_T(\text{aq})$  as a function of time? For IDMP, MIDA and PMG,  $\text{Mn}_T(\text{aq})$  increases over time; the efficiency of  $\text{Mn}_T(\text{aq})$  production decreases in the order: IDMP > MIDA > PMG.  $\text{MnOOH}$  gradually releases  $\text{Mn}_T(\text{aq})$ , even in the absence of chelating agent. When chelating agents are present, we will assume that the gradual release of  $\text{Mn}_T(\text{aq})$  just described proceeds in parallel. Adding IDA doesn't yield any

higher  $Mn_T(aq)$ , indicating that IDA does not cause  $MnOOH$  dissolution throughout 75 hours of reaction.

What can we say about  $Mn^{III}(aq)$  as a function of time for the three chelating agents that do dissolve  $MnOOH$ ? With IDMP,  $Mn^{III}(aq)$  increases very fast in the first 5 hours of reaction and levels out in the next 70 hours of reaction. With PMG,  $Mn^{III}(aq)$  levels out at one-tenth the value for IDMP. With MIDA,  $Mn^{III}(aq)$  stays below the detectable level. The relative  $Mn^{III}(aq)$  abundance is also illustrated in the CE electropherogram (Figure 5.8b):  $Mn^{III}(aq)$  peakarea with IDMP is much higher than with PMG, no  $Mn^{III}(aq)$  peak is detected with MIDA, in spite of similar  $Mn_T(aq)$  values with all three chelating agents.

Note that  $Mn^{III}(aq)$  and  $Mn^{II}(aq)$  are the reminiscence of ligand-assisted dissolution and reductive dissolution, respectively. Our experimental results indicate that: IDMP leads to predominant ligand-assisted dissolution; MIDA leads to exclusive reductive dissolution; PMG leads to the mixed dissolution, in which the ligand-assisted dissolution is about 10-times less efficient than that of IDMP; IDA does not bring about dissolution.

## 5.5 Discussion

**5.5.1 Nonlinear Dissolution Kinetics.** In the Introduction section, a widely accepted dissolution kinetic model proposed by Stumm and co-workers has been presented (Equation 7), i.e. the dissolution rate ( $R_L$ ) and the concentration of surface precursor complexes ( $C_L^s$ ) follow a linear relationship (34, 35). Their model also suggests that

once the surface is saturated by chelating agent, in which case  $C_L^s$  remains constant, the dissolution rate should be independent of the added chelating agent concentration.

The results obtained in this study, however, show nonlinear dissolution kinetics for  $MnO_2$ -bound or  $MnOOH$ -bound  $Mn^{III}$  dissolution by PP, MDP, and PAA. The decrease in dissolution rate has been attributed to surface heterogeneity and the reduction of surface area by Stumm and co-workers (35). Lin and Benjamin (25) added that a backward reaction opposing the detachment step may also contribute to a decrease in dissolution rate. Considering the backward reaction hypothesis to this study, we can visualize that dissolved  $Mn^{III}$  complexes may return to the surface via precipitation or adsorption. The backward reaction grows in importance as the reaction proceeds and hence causes the decrease in rate.

As far as the leveling out  $Mn^{III}(aq)$  concentration is concerned, experimental results from the effect of  $MnO_2$  loading indicate that for the loading of 200  $\mu M$  oxide, 5.0 mM PP, MDP and PAA, leveling out  $Mn^{III}(aq)$  concentration is not limited by thermodynamic controls presented in Equation 11. Leveling out  $Mn^{III}(aq)$  concentration is, on the other hand, more likely controlled by surface reactions.

**5.5.2 Comparisons among Group I Chelating Agents.** Chelating agent functional groups and structure affect ligand-assisted dissolution from three aspects: (i) concentration and nature of surface precursor complexes, (ii) susceptibility of detaching surface-bound  $Mn^{III}$ -complexes reflected by dissolution rate coefficient, (iii) the equilibrium constants ( $\log K_s$ ) for  $Mn^{III}$  complexation in solution. Based on the assumption that dissolution is surface reaction controlled, dissolution rate will be affected by aspects (i) and (ii). The  $\log K_s$  described in aspect (iii) establishes the thermodynamic

constraint for ligand-assisted dissolution, i.e. whether a chelating agent is thermodynamically capable of solubilizing appreciable concentrations of  $\text{Mn}^{\text{III}}$ . Besides, as Ludwig et. al (36) have found out in their study, the logKs for metal complexation in solution correlate well with the dissolution rate coefficients. Their study indicates that, in some cases, the activated surface complexes are analogous to the analogous dissolved complexes in important ways (36).

Precursor complexes with suitable coordinative arrangement are crucial to promote dissolution. The exact nature of this precursor complex is not at present known. Precursor complex formation may be outer-sphere or inner-sphere. Inner sphere complexes may be either monodentate or bidentate (coordination via one or both Lewis Base groups). Bidentate complexes may be mononuclear (involving only one surface-bound  $\text{Mn}^{\text{III}}$  atom) or binuclear (oxalate may bridge between neighboring  $\text{Mn}^{\text{III}}$  atoms). As far as dissolution is concerned, bidentate (or multidentate) mononuclear surface chelates are believed to be more effective in enhancing dissolution rate than monodentate surface complexes (36, 37). The chelate ring size is critical, with 5- and 6-membered ring more effective in promoting dissolution (34, 37, 38). Binuclear species inhibit dissolution because the simultaneous removal of two metal centers is energetically unfavorable (37).

Similar to the above mentioned studies (36, 37), Group I chelating agent-assisted  $\text{Mn}^{\text{III}}$  dissolution can be predicted from their complexation in solution. It has been unambiguously determined by both potentiometric titration and  $^{31}\text{P}$ -NMR that PP forms 6-membered chelate rings with dissolved metal ions that involve oxygen Lewis Base groups from both phosphate arms of the molecule (39). We will assume that MDP and



PAA also form 6-membered rings with dissolved metal ions. EDP and PPA possess a structure with the potential to form a 7-membered ring with dissolved metal ions. MP, bearing a single phosphonate group, does not form a ring structure with metal ions in solution (40). From the chemistry of solution phase coordination, we can predict that the surface  $\text{Mn}^{\text{III}}$  complexation with EDP, PPA and MP should be much weaker than that of PP, MDP and PAA. Not surprisingly, EDP, PPA and MP do not yield appreciable  $\text{Mn}^{\text{III}}(\text{aq})$ . PP, MDP and PAA, on the other, do yield appreciable  $\text{Mn}^{\text{III}}(\text{aq})$ .

Replacing a carboxylate group with a phosphonate group generally increases logKs for complex formation, owing to higher charge and higher basicity (41). The fact that PAA yields both less initial and leveling-out concentrations of  $\text{Mn}^{\text{III}}(\text{aq})$  than that of MDP and PP is in agreement with the idea that PAA is the weakest chelating agent for  $\text{Mn}^{\text{III}}$  among the three.

PBTC is the only group I chelating agent undergoes both ligand-assisted dissolution and electron-transfer reaction. PBTC consists of a PAA moiety in its structure, which may contribute to ligand-assisted dissolution. However, the two extra carboxylate arms may be a barrier in promoting dissolution, leading to  $\text{Mn}^{\text{III}}(\text{aq})$  released by PBTC only one-half that of PAA. They also make PBTC more subject to electron transfer reaction than PAA. PBTC-assisted dissolution exhibits non-linear dissolution kinetics. Because the rate of ligand-assisted dissolution slows down as reaction proceeds, the competitive electron transfer reaction starts to grow in importance. The electron transfer reaction may occur via intramolecular degradation within  $\text{Mn}^{\text{III}}$ -PBTC complexes in solution and/or reductive dissolution of surface  $\text{Mn}^{\text{III,IV}}$ . The fact that  $\text{Mn}_{\text{T}}(\text{aq})$  is eventually higher than  $\text{TOTMn}^{\text{III}}$  indicates dissolution via reduction of  $\text{Mn}^{\text{IV}}$  takes place.

**5.5.3 Comparisons among Group II Chelating Agents.** Group II chelating agents possess one N donor from amine group, and two O donors from carboxylate and/or phosphonate groups. In solution, the chelating agents coordinate with transition metal ions through (N,O) Lewis Base groups, resulting in forming two 5-membered chelating rings (41, 42). Titration studies show that the logKs for complex formation increase in the order: IDA < PMG < IDMP (15), which supports the idea that replacing a carboxylate group with a phosphonate group increases logKs. MIDA and IDA have identical Lewis Base groups, and hence it is plausible to assume that they have similar logKs for metal complexation. If the chemistry of solution phase coordination also applies for that of surface coordination, under our experimental condition, the logKs of Group II chelating agents for surface Mn<sup>III</sup> complexation should be high enough to yield appreciable Mn<sup>III</sup>(aq) thermodynamically.

Whereas the amine Lewis Base group is beneficial in the coordination of metal ions in solution, adsorption studies by several groups (43-45) suggest that, for predominant adsorbed species, the amine group in IDA, MIDA, and PMG does not participate in surface complexation. Hence, the strong chelate ring structures favored in solution are not favored on the surface. It is not surprising that IDA does not bring about dissolution. As we have observed for Group I chelating agents, a phosphonate group has stronger ability to promote Mn<sup>III</sup> dissolution than a carboxylate group. This is true also for Group II chelating agents, where the ability to promote Mn<sup>III</sup> dissolution increases in the order IDA, MIDA < PMG < IDMP. Because IDA and MIDA have identical Lewis Base groups, they should adsorb to nearly identical extents. Like IDA, MIDA should not bring about ligand-assisted dissolution. The release of Mn<sup>II</sup>(aq) by MIDA is most likely

caused by reductive dissolution. The release of  $\text{Mn}^{\text{II}}(\text{aq})$  by PMG, on the other hand, may be caused by reductive dissolution as well as intramolecular electron transfer within dissolved  $\text{Mn}^{\text{III}}$ -PGM complexes. IDMP is resistant to oxidation, and leads to ligand-assisted dissolution as the dominant pathway.

## 5.6 Literature Cited

- (1) Luther, G. W., Nuzzio, D. B., and Wu, J. F. Speciation of manganese in chesapeake bay waters by voltammetric methods. *Analytica Chimica Acta* **1994**, 284, 473-480.
- (2) Kostka, J. E., Luther, G. W., and Nealson, K. H. Chemical and biological reduction of  $\text{mn(III)}$ -pyrophosphate complexes - potential importance of dissolved  $\text{mn(III)}$  as an environmental oxidant. *Geochimica Et Cosmochimica Acta* **1995**, 59, 885-894.
- (3) Klewicki, J. K. and Morgan, J. J. Kinetic behavior of  $\text{mn(III)}$  complexes of pyrophosphate, edta, and citrate. *Environ. Sci. Technol.* **1998**, 32, 2916-2922.
- (4) Klewicki, J. K. and Morgan, J. J. Dissolution of  $\beta$ - $\text{mnooh}$  particles by ligands: Pyrophosphate, ethylenediaminetetraacetate, and citrate. *Geochimica et Cosmochimica Acta* **1999**, 63, 3017-3024.
- (5) Luther, G. W., Ruppel, D. T., and Burkhard, C. A. Reactivity of dissolved  $\text{mn(III)}$  complexes and  $\text{mn(IV)}$  species with reductants: Mn redox chemistry without a dissolution step? In *Mineral-water interfacial reactions: Kinetics and mechanisms*, D.L. Sparks and T.J. Grundl, Editors. 1999, American Chemical Society: Washington, DC. 265-280.
- (6) Parker, D. L., Sposito, G., and Tebo, B. M. Manganese(III) binding to a pyoverdine siderophore produced by a manganese(II)-oxidizing bacterium. *Geochimica Et Cosmochimica Acta* **2004**, 68, 4809-4820.
- (7) Duckworth, O. W. and Sposito, G. Siderophore-manganese(III) interactions. I. Air-oxidation of manganese(II) promoted by desferrioxamine b. *Environmental Science & Technology* **2005**, 39, 6037-6044.
- (8) Duckworth, O. W. and Sposito, G. Siderophore-manganese(III) interactions ii. Manganite dissolution promoted by desferrioxamine b. *Environmental Science & Technology* **2005**, 39, 6045-6051.
- (9) Webb, S. M., Dick, G. J., Bargar, J. R., and Tebo, B. M. Evidence for the presence of  $\text{mn(III)}$  intermediates in the bacterial oxidation of  $\text{mn(II)}$ . *Proceedings*

*of the National Academy of Sciences of the United States of America* **2005**, 102, 5558-5563.

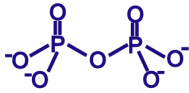
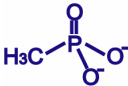
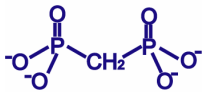
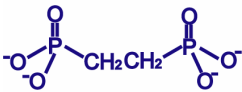
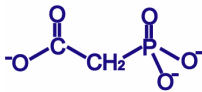
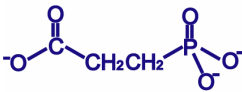
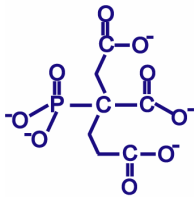
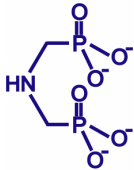
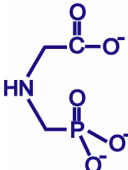
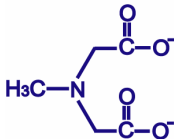
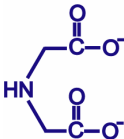
- (10) Kuan, I. C., Johnson, K. A., and Tien, M. Kinetic-analysis of manganese peroxidase - the reaction with manganese complexes. *Journal of Biological Chemistry* **1993**, 268, 20064-20070.
- (11) Roy, B. P., Paice, M. G., Archibald, F. S., Misra, S. K., and Misiak, L. E. Creation of metal-complexing agents, reduction of manganese-dioxide, and promotion of manganese peroxidase-mediated mn(iii) production by cellobiose - quinone oxidoreductase from *trametes-versicolor*. *Journal of Biological Chemistry* **1994**, 269, 19745-19750.
- (12) Schlosser, D. and Hofer, C. Laccase-catalyzed oxidation of  $\text{mn}^{2+}$  in the presence of natural  $\text{mn}^{3+}$  chelators as a novel source of extracellular  $\text{h}_2\text{o}_2$  production and its impact on manganese peroxidase. *Applied and Environmental Microbiology* **2002**, 68, 3514-3521.
- (13) Knocke, W. R., Occiano, S. C., and Hungate, R. Removal of soluble manganese by oxide-coated filter media - sorption rate and removal mechanism issues. *Journal American Water Works Association* **1991**, 83, 64-69.
- (14) Sugam, R., Garey, J. F., and White, J. M. Chapter 42: Manganese deposition in chlorinated power plant cooling water. In *Water chlorination: Chemistry, environmental impact, and health effects*, R.L. Jolley, et al., Editors. 1990, Lewis Publishers: Chelsea, MI.
- (15) Motekaitis, R. J. and Martell, A. E. Metal chelate formation by n-phosphonomethylglycine and related ligands. *Journal of Coordination Chemistry* **1985**, 14, 139-149.
- (16) Barja, B. C. and Afonso, M. D. An atr-ftir study of glyphosate and its  $\text{fe}(\text{iii})$  complex in aqueous solution. *Environmental Science & Technology* **1998**, 32, 3331-3335.
- (17) Kiely, T., Donaldson, D., and Grube, A. *Pesticides industry sales and usage-2000 and 2001 market estimates*. 2004, Biological and Economic Analysis Division, Office of Pesticide Programs, Office of Prevention, Pesticides, and Toxic Substances, U.S. Environmental Protection Agency: Washington, DC. 14.
- (18) Nowack, B. The behavior of phosphonates in wastewater treatment plants of switzerland. *Water Research* **1998**, 32, 1271-1279.
- (19) Ridge, A. C. and Sedlak, D. L. Effect of ferric chloride addition on the removal of  $\text{cu}$  and  $\text{zn}$  complexes with edta during municipal wastewater treatment. *Water Research* **2004**, 38, 921-932.

- (20) Tomson, M. B., Kan, A. T., and Oddo, J. E. Acid-base and metal-complex solution chemistry of the polyphosphonate dtpmp versus temperature and ionic-strength. *Langmuir* **1994**, 10, 1442-1449.
- (21) Chiarizia, R. and Horwitz, E. P. New formulations for iron-oxides dissolution. *Hydrometallurgy* **1991**, 27, 339-360.
- (22) McArdell, C. S., Stone, A. T., and Tian, J. Reaction of edta and related aminocarboxylate chelating agents with coiiiiooh (heterogenite) and mniiiiooh (manganite). *Environ. Sci. Technol.* **1998**, 32, 2923-2930.
- (23) Nowack, B. and Stone, A. T. Homogeneous and heterogeneous oxidation of nitrilotrismethylenephosphonic acid (ntmp) in the presence of manganese (ii, iii) and molecular oxygen. *J. Phys. Chem. B* **2002**, 106, 6227-6233.
- (24) Stumm, W. *Chemistry of the solid-water interface: Processes at the mineral-water and particle-water interface in natural systems*. 1992, New York: John Wiley.
- (25) Lin, C. F. and Benjamin, M. M. Dissolution kinetics of minerals in the presence of sorbing and complexing ligands. *Environmental Science & Technology* **1990**, 24, 126-134.
- (26) Luo, J. A., Zhang, Q. H., and Suib, S. L. Mechanistic and kinetic studies of crystallization of birnessite. *Inorganic Chemistry* **2000**, 39, 741-747.
- (27) Wang, Y. and Stone, A. T. The citric acid-mniii,ivo2(birnessite) reaction. Electron transfer, complex formation, and autocatalytic feedback. *Submitted to Geochimica Et Cosmochimica Acta* **2005**.
- (28) Giovanoli, R. and Leuenberger, U. Oxidation of manganese oxide hydroxide. *Helvetica Chimica Acta* **1969**, 52, 2333-2347.
- (29) Wang, Y. and Stone, A. T. Reaction of mniii,iv (hydr)oxides with oxalic acid, glyoxylic acid, phosphonoformic acid, and structurally-related organic compounds. *Submitted to Geochimica Et Cosmochimica Acta*.
- (30) Carbonaro, R. F. and Stone, A. T. Speciation of chromium(iii) and cobalt(iii) (amino)carboxylate complexes using capillary electrophoresis. *Analytical Chemistry* **2005**, 77, 155-164.
- (31) Burgisser, C. S. and Stone, A. T. Determination of edta, nta, and other amino carboxylic acids and their co(ii) and co(iii) complexes by capillary electrophoresis. *Environmental Science & Technology* **1997**, 31, 2656-2664.
- (32) Cotton, F. A., Wilkinson, G., Murillo, C. A., and Bochmann, M. *Advanced inorganic chemistry*. 6th ed. 1999, New York: Wiley Interscience. 757-775.

- (33) Shriver, D., and Atkins, P. *Inorganic chemistry*. 3rd ed. 1999, New York: W.H. Freeman and Company. 190.
- (34) Furrer, G. and Stumm, W. The coordination chemistry of weathering .1. Dissolution kinetics of delta-al<sub>2</sub>O<sub>3</sub> and beo. *Geochimica Et Cosmochimica Acta* **1986**, 50, 1847-1860.
- (35) Stumm, W. and Wollast, R. Coordination chemistry of weathering - kinetics of the surface-controlled dissolution of oxide minerals. *Reviews of Geophysics* **1990**, 28, 53-69.
- (36) Ludwig, C., Casey, W. H., and Rock, P. A. Prediction of ligand-promoted dissolution rates from the reactivities of aqueous complexes. *Nature* **1995**, 375, 44-47.
- (37) Stumm, W. Reactivity at the mineral-water interface: Dissolution and inhibition. *Colloids and Surfaces a-Physicochemical and Engineering Aspects* **1997**, 120, 143-166.
- (38) Duckworth, O. W. and Martin, S. T. Surface complexation and dissolution of hematite by c-1-c-6 dicarboxylic acids at ph=5.0. *Geochimica Et Cosmochimica Acta* **2001**, 65, 4289-4301.
- (39) Atkari, K., Kiss, T., Bertani, R., and Martin, R. B. Interactions of aluminum(iii) with phosphates. *Inorganic Chemistry* **1996**, 35, 7089-7094.
- (40) Barja, B. C., Herszage, J., and Alfonso, M. D. Iron(iii)-phosphonate complexes. *Polyhedron* **2001**, 20, 1821-1830.
- (41) Kiss, T. and Lazar, I. Structure and stability of metal complexes in solution. In *Aminophosphonic and aminophosphinic acids*, V.P. Kukhar and H.R. Hudson, Editors. 2000, Wiley: New York. 284-323.
- (42) Dwyer, F. P. and Mellor, D. P. *Chelating agents and metal chelates*. 1964, New York: Academic Press.
- (43) Sheals, J., Sjoberg, S., and Persson, P. Adsorption of glyphosate on goethite: Molecular characterization of surface complexes. *Environmental Science & Technology* **2002**, 36, 3090-3095.
- (44) Whitehead, C. F. *Speciation of carboxylate-containing chelating agent in the presence of iron (hydr)oxide minerals and metal ions*. 2003, The Johns Hopkins University: Baltimore, MD.
- (45) Ramstedt, M., Norgren, C., Sheals, J., Shchukarev, A., and Sjoberg, S. Chemical speciation of n-(phosphonomethyl)glycine in solution and at mineral interfaces. *Surface and Interface Analysis* **2004**, 36, 1074-1077.

- (46) Martell, A. E., Smith, R. M., and Motekaitis, R. J. *Nist critically selected stability constants of metal complexes database*. 2004, US Department of Commerce, National Institute of Standards and Technology: Gaithersburg, MD.
- (47) Valle, A., China, E., Dominguez, S., Mederos, A., Midollini, S., and Vacca, A. Complexes of beryllium(ii) in aqueous solution with 3-phosphonopropionic acid. *Polyhedron* **1999**, 18, 3253-3256.
- (48) Salvado, V., Escoda, L., and de la Torre, F. A study of the complex formation between trivalent ions ( $\text{Al}^{3+}$ ,  $\text{Fe}^{3+}$ ) and 2-phosphonobutane-1,2,4-tricarboxylic acid and their industrial applications. *Polyhedron* **1999**, 18, 3275-3280.

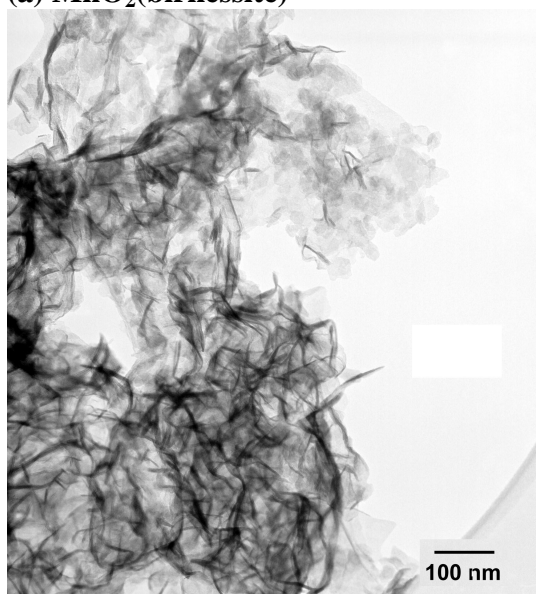
**Table 5.1. Chelating Agents Employed in This Study**

Name	pK <sub>a</sub> <sup>1</sup>	Structure	Name	pK <sub>a</sub> <sup>1</sup>	Structure
<b>Group I Chelating Agents</b>					
PP	0.9 2.28 6.70 9.40		MP	2.32 8.00	
MDP	1.82 2.96 7.40 10.96		EDP	1.5 3.18 7.62 9.28	
PAA	1.3 5.11 8.60		PPA	2.12 <sup>2</sup> 5.07 <sup>2</sup> 8.56 <sup>2</sup>	
PBTC	4.05 <sup>3</sup> 4.86 <sup>3</sup> 6.08 <sup>3</sup> 8.06 <sup>3</sup> 10.62 <sup>3</sup>				
<b>Group II Chelating Agents</b>					
IDMP	0.8 1.4 5.51 6.74 11.64		PMG	0.7 <sup>4</sup> 2.40 5.90 10.82	
MIDA	2.12 2.59 10.01		IDA	1.85 2.84 9.79	

<sup>1</sup>Unless otherwise noted, pK<sub>a</sub> values are for 25°C and infinite dilution conditions (ionic strength = 0), and were obtained from the CRITICAL (46) database. <sup>2</sup>from Valle et al. (47) <sup>3</sup>from Salvado et al. (48) <sup>4</sup>from the CRITICAL (46) database, pK<sub>a</sub> value obtained at 20 °C



**(a)  $\text{MnO}_2$ (birnessite)**



**(b)  $\text{MnOOH}$ (manganite)**

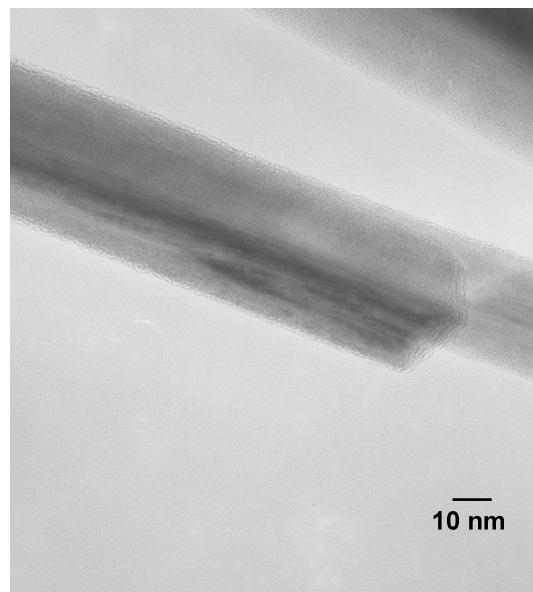
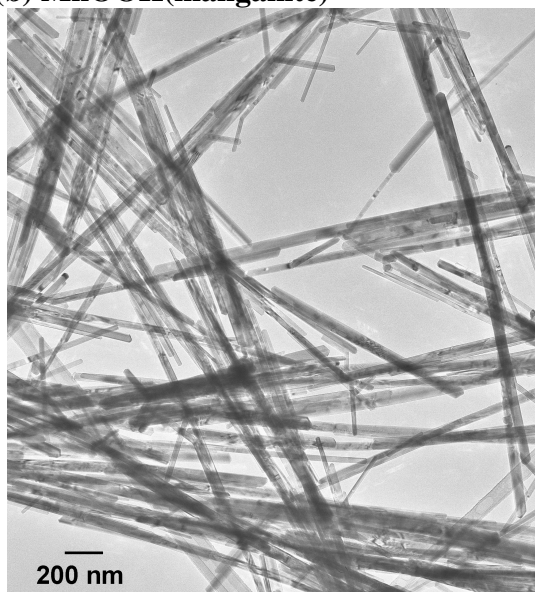


**Figure 5.1. Transmission electron micrographs of (a)  $\text{MnO}_2$ (birnessite) and (b)  $\text{MnOOH}$ (manganite) employed in this study.**

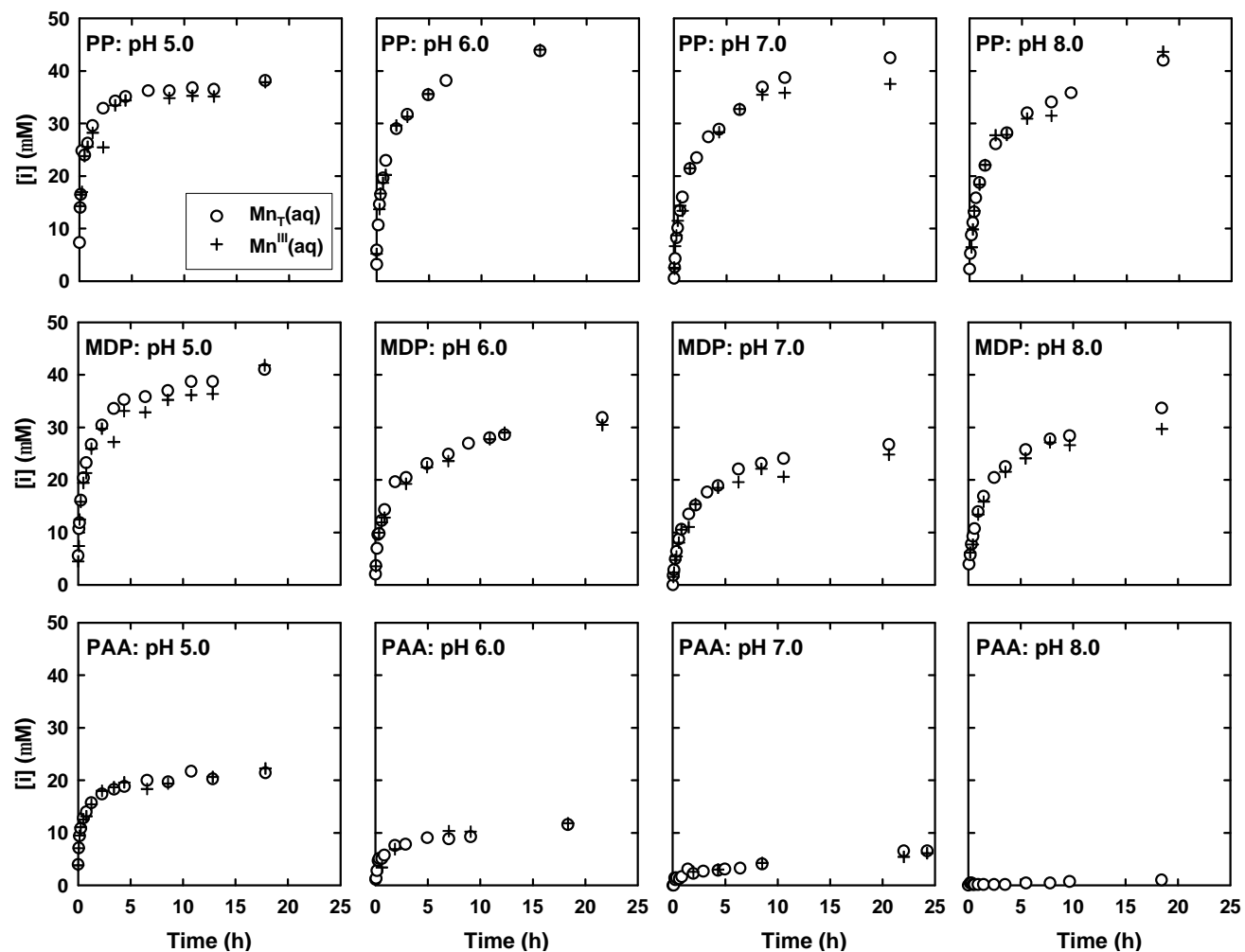


**Figure 5.2.** Time course plots at different pH values for reaction of 200 mM  $\text{MnO}_2$  with 5.0 mM PP (top panels), MDP (middle panels), and PPA (bottom panels). A pH stat was employed at pH 6.0, 7.0, and 8.0 for reactions with MDP and PAA. For all other experiments, self-buffering was sufficient to maintain constant pH.

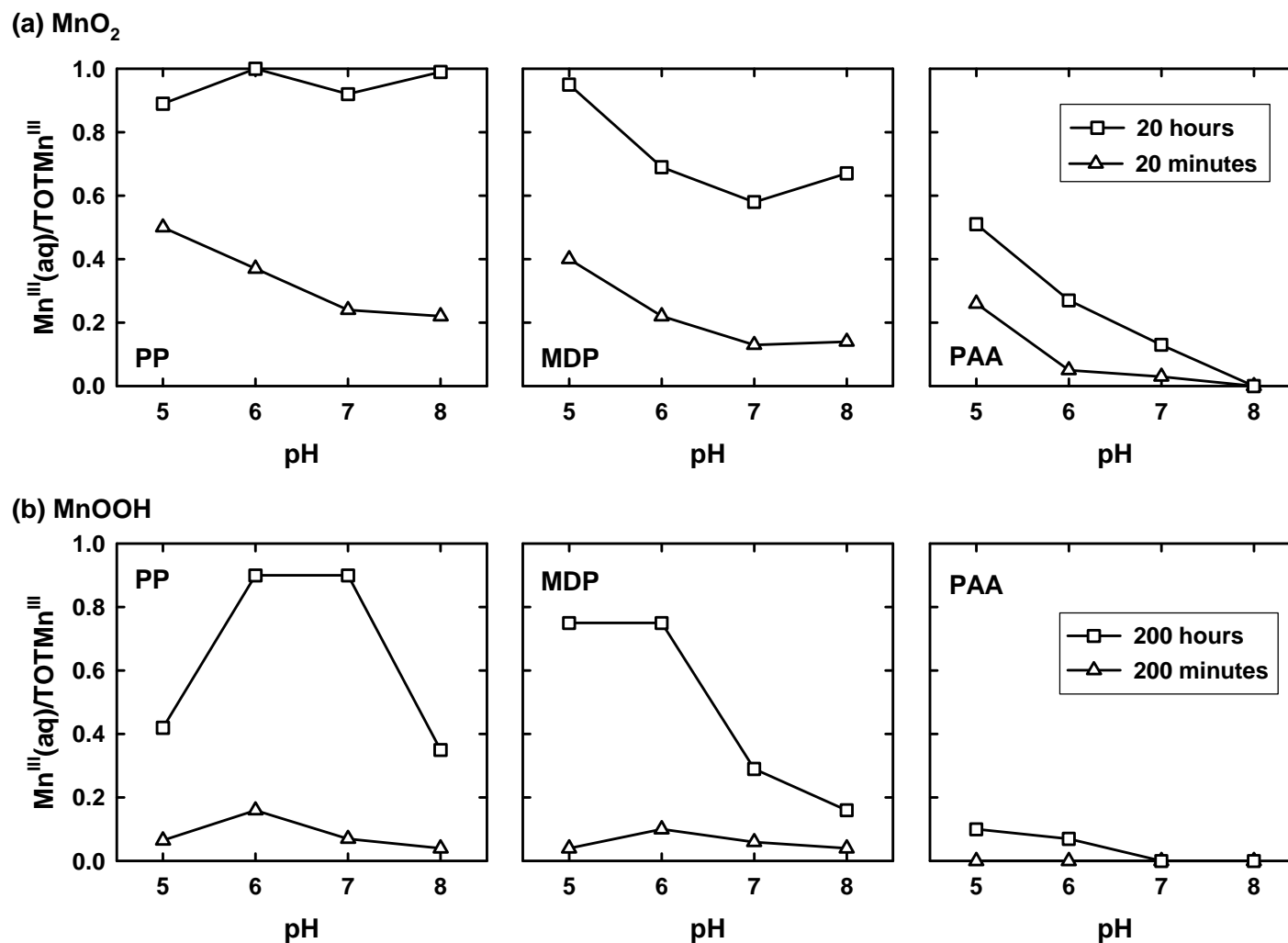
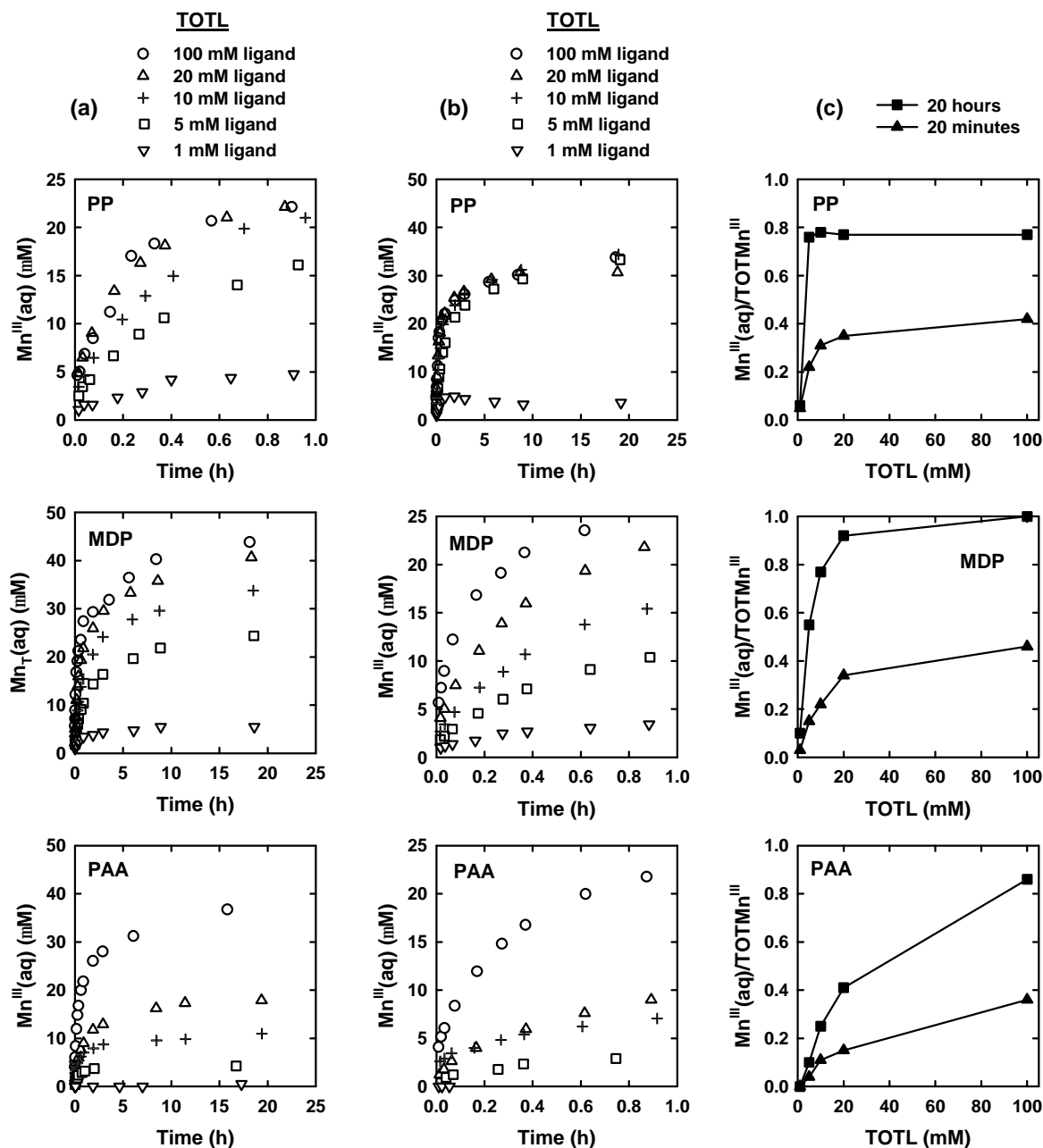


Figure 5.3. Fraction of  $\text{TOTMn}^{\text{III}}$  dissolved as a function of chelating agent concentration based on time course plots presented in (a) Figure 5.2 and (b) Figure 5.6. Fraction dissolved is shown after 20 minutes and after 20 hours of reaction.



**Figure 5.4. Effect of PP, MDP, and PAA concentration on dissolution of 200 mM MnO<sub>2</sub> at pH 7.0. (a) and (b): Time course plots of Mn<sup>III</sup>(aq) concentration for the first 1 hour and 25 hours, respectively. (c): Fraction of TOTMn<sup>III</sup> dissolved as a function of chelating agent concentration. Fraction dissolved is shown after 20 minutes and after 20 hours of reaction. A pH stat was employed for all experiments with PAA, and for 1.0 mM concentrations of PP and MDP. Self-buffering maintained constant pH with higher concentrations of PP and MDP.**

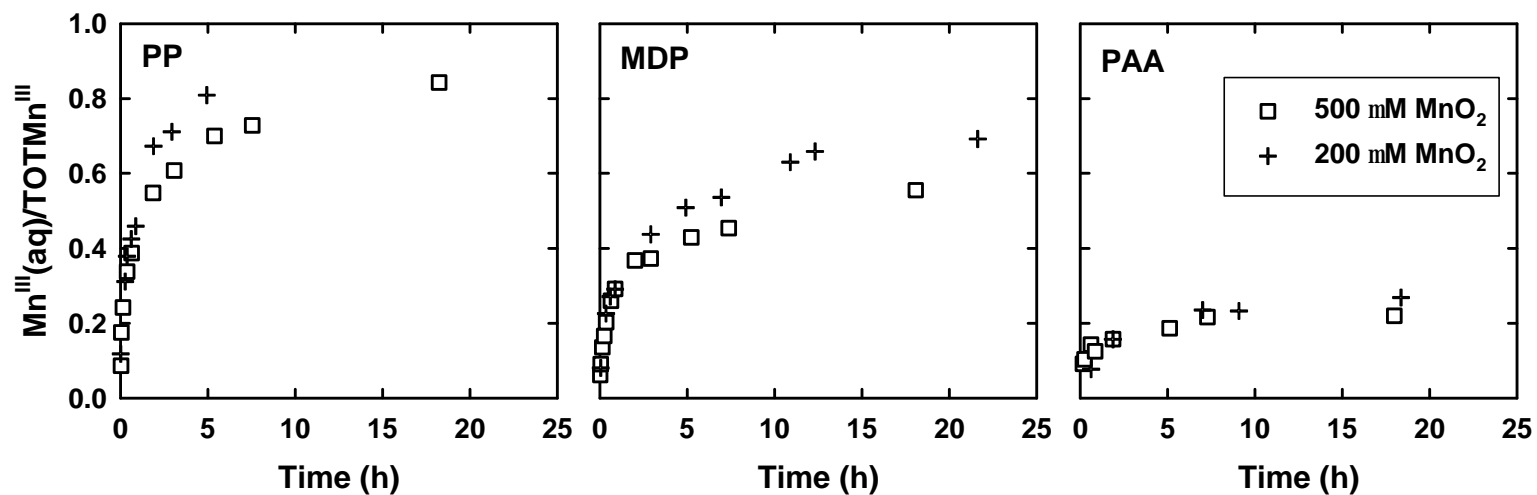
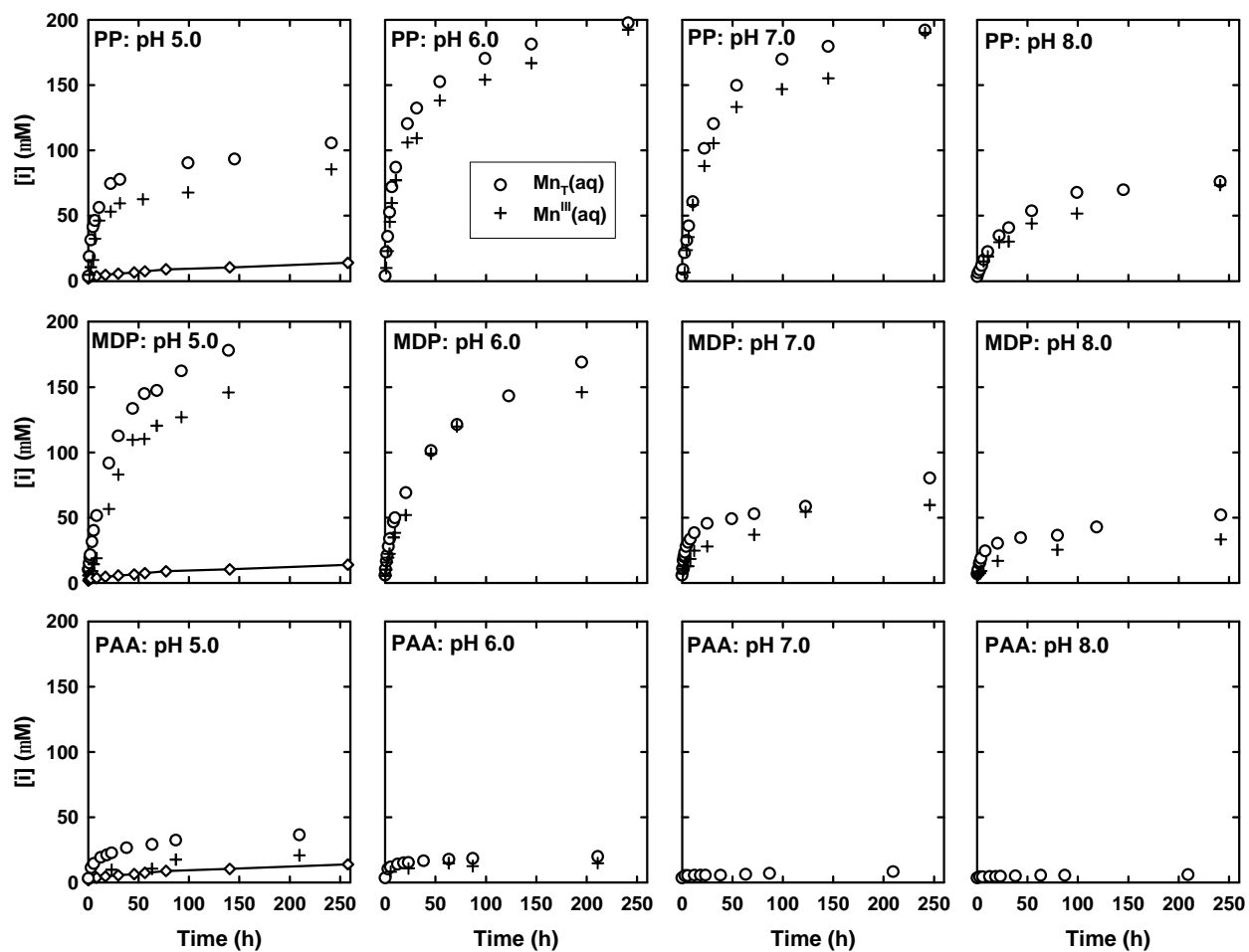
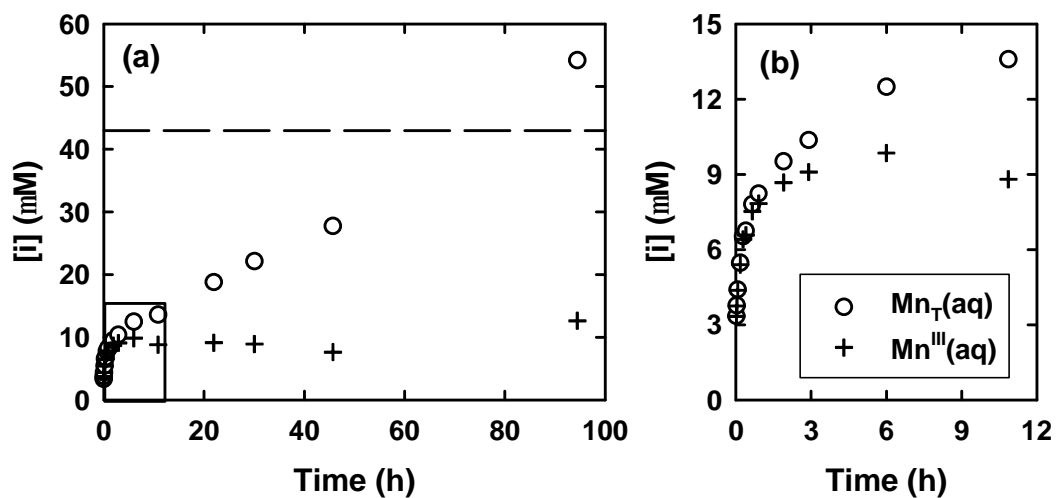


Figure 5.5. Effect of MnO<sub>2</sub> loading on times course plots at pH 6.0 (5.0 mM PP, MDP, and PPA). For all experiments, self-buffering was sufficient to maintain constant pH.



**Figure 5.6.** Time course plots at different pH values for reaction of 200 mM MnOOH with 5.0 mM PP (top panels), MDP (middle panels), and PPA (bottom panels). A pH stat was employed at pH 5.0 for reactions without chelating agent and with MDP, at pH 7.0 for reaction with PAA. For all other experiments, self-buffering was sufficient to maintain constant pH. The symbol -à- in the pH 5.0 plots (left panels) represents  $\text{Mn}_T(\text{aq})$  released without chelating agents.



**Figure 5.7. (a) Dissolution of 200 mM  $\text{MnO}_2$  by 5.0 mM PBTC at pH 5.0. (b) Close-up of the first 12 hours of reaction. Self-buffering by PBTC was sufficient to maintain constant pH.**

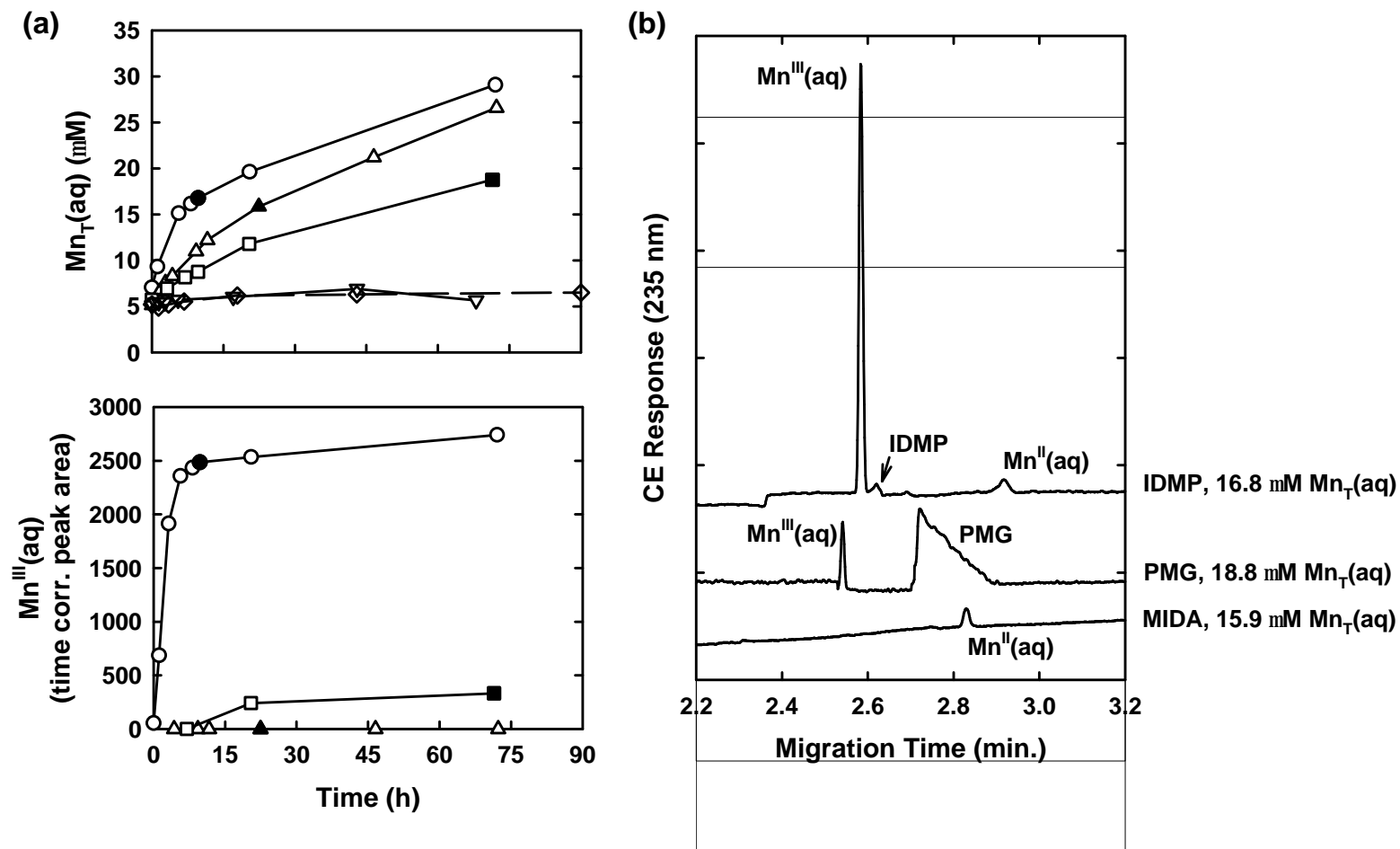


Figure 5.8. (a) Time course plots for reaction of 200 mM  $MnOOH$  with 5.0 mM chelating agents at pH 6.0 with respect to  $Mn_T(aq)$  (top plot) and  $Mn^{III}(aq)$  (bottom plot) production. pH maintained by self-buffering effect for IDMP and PMG, by pH stat for MIDA and IDA. The symbol - $\Delta$ - corresponds to  $Mn_T(aq)$  released without adding chelating agent. (b) Electropherograms of filtered sample solutions corresponding to filled symbols in time course plots.